

Chapter 4

SYSTEM MODELING OF AN MIP

The dynamics of an MIP has to be described by a mathematical model in order to facilitate the development of an efficient control system for the balancing of the inverted pendulum and rotation the MIP. In this chapter, the equation of motion for the MIP and the linear model of a DC motor are derived in detail.

4.1 Linear Model of a DC Motor

The MIP is driven by two Faulhaber DC motors. The state-space model of the DC motor will be derived in this section. This model will be used in the dynamic model of the balancing MIP to provide a relationship between the input voltage to the motors and the control torque needed to balance the MIP.

To determine the mathematical model of the DC motor, we use the diagram of a DC motor as shown in Figure 4.1. where

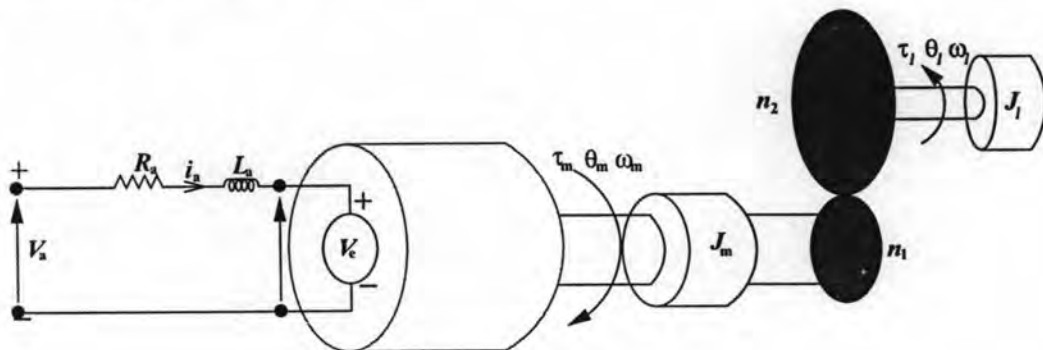


Figure 4.1: Diagram of a DC motor with gear box.

V_a is armature circuit input voltage (V)

R_a is armature resistance (Ω)

L_a is armature inductance (H)

i_a is armature circuit current (A)

V_e is motor back-emf voltage (V)

τ_m is torque generated by the motor (N-m)

τ_l is torque applied at the load (N-m)

J_m is motor moment of inertia (kg-m^2)

J_l is moment of inertia of the load connected to the shaft (kg-m^2)

θ_m is motor shaft position (rad)

θ_l is load shaft position (rad)

ω_m is motor shaft angular velocity (rad/s)

ω_l is load shaft angular velocity (rad/s)

n_1, n_2 are teeth numbers of the gears

When a voltage is applied to the terminals of the motor, a current i_a is generated in the motor armature. The motor produces a torque τ_m , which is proportional to the current. This relationship can be expressed as

$$\tau_m = \eta_m K_m i_a \quad (4.1)$$

where

K_m Motor-torque constant (N-m/A)

η_m Motor efficiency

A resistor-inductor pair in series with a voltage, V_e , can be used to model the electrical circuit of the motor. This back electromotive force voltage is produced because the coils of the motor are moving through a magnetic field. The voltage produced can be approximated as a linear function of shaft velocity, which can be written as

$$V_e = K_e \omega_m \quad (4.2)$$

where

K_e is back-emf constant (V-s/rad)

At this point, a linear differential equation for the DC motor's electrical circuit can be written by using *Kirchhoff's Voltage Law*, the law states that the sum of all voltages in the circuit must equal to zero. For the DC motor, this can be written as

$$V_a - R_a i_a - L_a \frac{di_a}{dt} - V_e = 0 \quad (4.3)$$

Since $L_a \ll R_a$, we can disregard the motor inductance leaving us with

$$i_a = \frac{V_a - V_e}{R_a} \quad (4.4)$$

Substituting equation (4.2) into equation (4.4) we get

$$i_a = \frac{V_a - K_e \omega_m}{R_a} \quad (4.5)$$

We now shift over to the mechanical aspect of the motor and begin by applying Newton's second law of motion to the motor shaft to get

$$J_m \frac{d\omega_m}{dt} = \tau_m - \frac{\tau_l}{\eta_g K_g} \quad (4.6)$$

where $\frac{\tau_l}{\eta_g K_g}$ is the load torque seen through the gears, η_g is the efficiency of the gearbox, and $K_g = \frac{n_2}{n_1}$ is the gear ratio.

The second law of motion is applies at the load of the motor to get

$$J_l \frac{d\omega_l}{dt} = \tau_l - B_{cq} \omega_l \quad (4.7)$$

where B_{cq} is the equivalent viscous damping coefficient as seen at the output.

Substituting (4.6) into (4.7), we are left with

$$J_l \frac{d\omega_l}{dt} = \eta_g K_g \tau_m - \eta_g K_g J_m \frac{d\omega_m}{dt} - B_{cq} \omega_l \quad (4.8)$$

Substituting $\dot{\theta} = \omega$ into equation (4.8), we can rewrite it as

$$J_l \ddot{\theta}_l = \eta_g K_g \tau_m - \eta_g K_g J_m \ddot{\theta}_m - B_{cq} \dot{\theta}_l \quad (4.9)$$

We know that $\theta_m = K_g \theta_l$ and substituting equation (4.1) into equation (4.9), we get

$$J_l \ddot{\theta}_l + \eta_g K_g^2 J_m \ddot{\theta}_l + B_{cq} \dot{\theta}_l = \eta_g \eta_m K_m K_g i_a \quad (4.10)$$

Finally, we can combine the electrical and mechanical equations by substituting (4.5) into (4.10) yielding

$$J_l \ddot{\theta}_l + \eta_g K_g^2 J_m \ddot{\theta}_l + B_{cq} \dot{\theta}_l = \eta_g \eta_m K_m K_g \frac{V_a - K_e \omega_m}{R_a} \quad (4.11)$$

This can be interpreted as the equivalent moment of inertia of the motor system as seen at the output.

Thus, the output torque on the load from the motor is

$$\tau_{\text{output}} = \eta_g \eta_m K_m K_g \frac{V_a - K_e K_g \dot{\theta}_1}{R_a} \quad (4.12)$$

We rearrange this equation as

$$\ddot{\theta}_1 = \frac{\eta_g \eta_m K_m K_g}{J_{\text{eq}} R_a} V_a - \left(\frac{\eta_g \eta_m K_m K_g^2 K_e}{J_{\text{eq}} R_a} + \frac{B_{\text{eq}}}{J_{\text{eq}}} \right) \dot{\theta}_1 \quad (4.13)$$

where $J_{\text{eq}} = J_l + \eta_g K_g^2 J_m$.

The motor's dynamics can be represented with a state-space model, it is a system of first order differential equations with position θ and velocity ω as states, that uniquely describe its operation. The inputs to the motor is then the applied voltage.

$$\begin{pmatrix} \dot{\theta}_1 \\ \dot{\omega}_1 \end{pmatrix} = \begin{pmatrix} 0 & 1 \\ 0 & -\left(\frac{B_{\text{eq}}}{J_{\text{eq}}} + \frac{\eta_g \eta_m K_m K_g^2 K_e}{J_{\text{eq}} R_a} \right) \end{pmatrix} \begin{pmatrix} \theta_1 \\ \omega_1 \end{pmatrix} + \begin{pmatrix} 0 \\ \frac{\eta_g \eta_m K_m K_g}{J_{\text{eq}} R_a} \end{pmatrix} V_a \quad (4.14)$$

$$y = \begin{pmatrix} 1 & 0 \end{pmatrix} \begin{pmatrix} \theta_1 \\ \omega_1 \end{pmatrix} \quad (4.15)$$

4.2 Identification of the DC Motor

The procedure of parameter identification of DC motor model using a method of recursive prediction error method, to identify the system through an experimental measuring of signals was carried out. PRBS signal is used as input and output of the system for identification is the motor angle (Figure 4.2). For the sampling period $t = 0.04s$ the following results of recorded input and output samples have been obtained. RPEM algorithm for identification of DC motor parameters is realized in MATLAB. The motor's dynamics can be represented with a state-space model as

$$\begin{pmatrix} \dot{\theta}_1 \\ \dot{\omega}_1 \end{pmatrix} = \begin{pmatrix} 0 & 1 \\ 0 & -368.9291 \end{pmatrix} \begin{pmatrix} \theta_1 \\ \omega_1 \end{pmatrix} + \begin{pmatrix} 0 \\ 180.4475 \end{pmatrix} V_a$$

$$y = \begin{pmatrix} 1 & 0 \end{pmatrix} \begin{pmatrix} \theta_1 \\ \omega_1 \end{pmatrix}$$

Figure 4.3 shows the comparison of the position and the velocity of the estimated model with those of the real system.

4.3 Dynamic Model for the MIP

The mobile inverted pendulum, albeit more complex in system dynamics, has similar behavior with a pendulum on a cart. The pendulum and wheel dynamics are analyzed separately

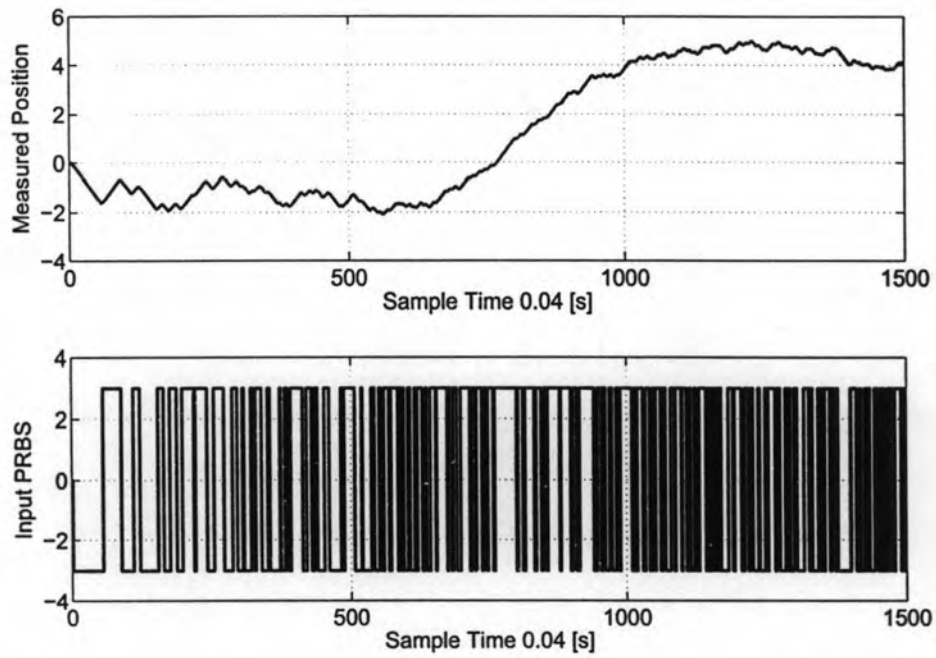


Figure 4.2: Measured input and output from DC motor via XPC-Target.

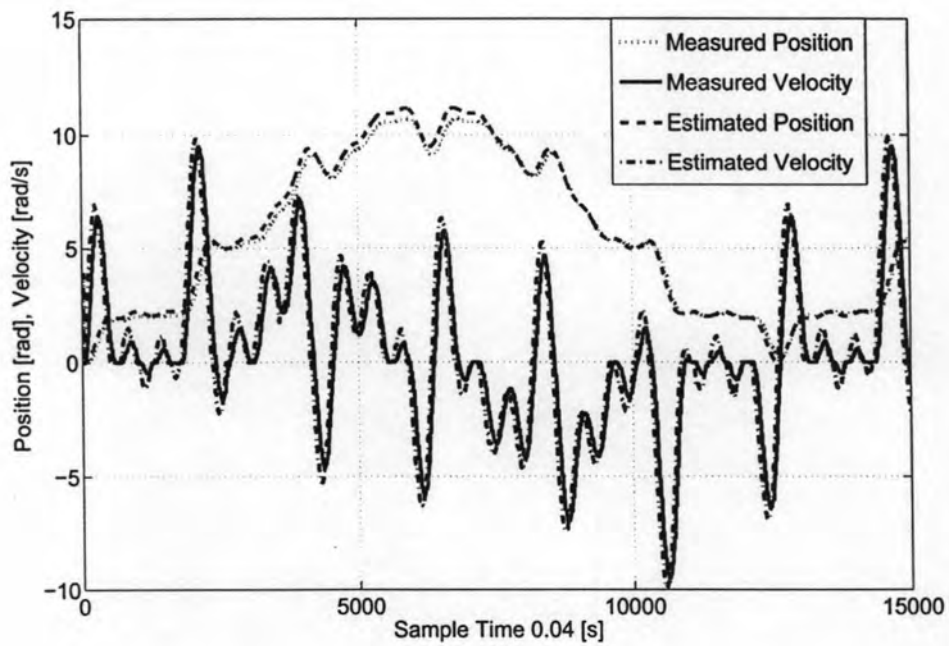


Figure 4.3: Comparing the model with a real system of a DC motor with gear.

at the beginning, but this will eventually lead to two equations of motion which completely describes the behavior of the balancing robot. As the robot's behavior can be influenced by disturbances as well as the torque from the motor, the mathematical model will have to accommodate such forces.

4.3.1 Dynamic Model of Two Wheels

For the right wheel

Firstly the equations of motion associated with the left and right wheels are obtained. Figure 4.4 shows the free body diagram for both wheels. Since the equation for the left and right wheels are completely analogous, only the equation for the right wheel is given.

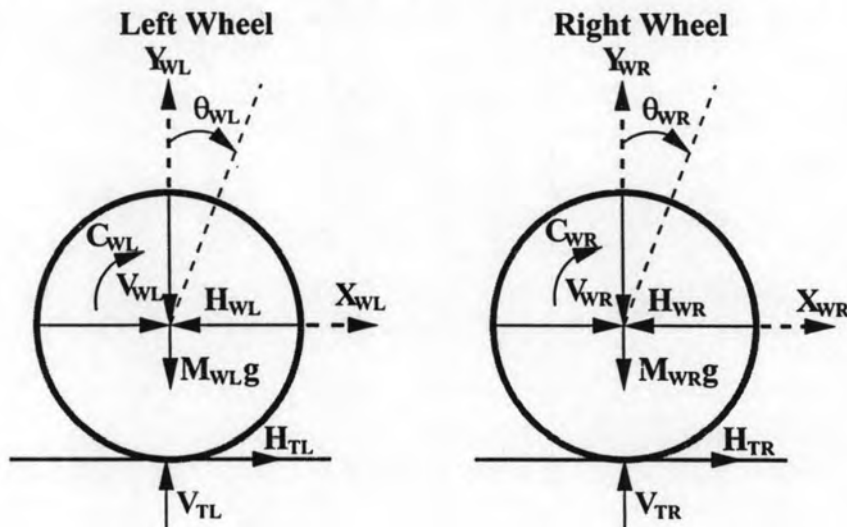


Figure 4.4: Free body diagram of the wheels.

θ_{WL}, θ_{WR} are rotation angle of the wheels (rad)

M_{WL}, M_{WR} are mass of the wheels (kg)

g Gravity constant (m/s^2)

$H_{WL}, H_{WR}, V_{WL}, V_{WR}$ are reaction forces between the wheel and chassis

C_{WL}, C_{WR} are applied torque from the motors to the wheels (N-m)

V_{TL}, V_{TR} are reaction forces between the ground and wheels

H_{TL}, H_{TR} are friction forces between the ground and wheels

r is radius of the wheels (m)

We assume that the mass, the moment of inertia and the angular rotation of two wheels are equals,

$$\begin{aligned} M_{WR} &= M_{WL} = M_W \\ J_{WR} &= J_{WL} = J_W \\ \theta_{WR} &= \theta_{WL} = \theta_W \end{aligned}$$

Using Newton's law of motion to the right wheel, the sum of forces on the horizontal x direction is

$$\begin{aligned} \sum F_x &= Ma \\ M_W \ddot{x} &= H_{TR} - H_{WR} \end{aligned} \quad (4.16)$$

And the sum of forces in y direction is

$$\begin{aligned} \sum F_y &= Ma \\ M_W \ddot{y} &= V_{TR} - M_{WR}g - V_{WR} \end{aligned} \quad (4.17)$$

Summing the forces around the center of the wheel gives

$$\begin{aligned} \sum M_O &= J\alpha \\ J_{eq} \ddot{\theta}_W &= C_{WR} - H_{TR}r \end{aligned} \quad (4.18)$$

From (4.12) the output torque to the wheel is attained

$$C_{WR} = \eta_g \eta_m K_m K_g \frac{V_{aR} - K_e K_g \dot{\theta}_W}{R_a}$$

Therefore, the equation (4.18) becomes

$$J_{eq} \ddot{\theta}_W = \frac{-\eta_g \eta_m K_m K_g^2 K_e}{R_a} \dot{\theta}_W + \frac{\eta_g \eta_m K_m K_g}{R_a} V_{aR} - H_{TR}r$$

Thus,

$$H_{TR} = \frac{-\eta_g \eta_m K_m K_g^2 K_e}{R_a r} \dot{\theta}_W + \frac{\eta_g \eta_m K_m K_g}{R_a r} V_{aR} - \frac{J_{eq}}{r} \ddot{\theta}_W \quad (4.19)$$

The equation (4.19) is substituted into (4.16) to get the equation for the right wheel

$$M_W \ddot{x} = \frac{-\eta_g \eta_m K_m K_g^2 K_e}{R_a r} \dot{\theta}_W + \frac{\eta_g \eta_m K_m K_g}{R_a r} V_{aR} - \frac{J_{eq}}{r} \ddot{\theta}_W - H_{WR} \quad (4.20)$$

Since the linear motion is acting on the center of the wheel, the angular rotation can be transformed into linear motion by simple transformation

$$\begin{aligned}\ddot{\theta}_W r &= \ddot{x} \implies \ddot{\theta}_W = \frac{\ddot{x}}{r} \\ \dot{\theta}_W r &= \dot{x} \implies \dot{\theta}_W = \frac{\dot{x}}{r}\end{aligned}$$

By the linear transformation, the equation (4.20) becomes

$$M_W \ddot{x} = \frac{-\eta_g \eta_m K_m K_g^2 K_c}{R_a r^2} \dot{x} + \frac{\eta_g \eta_m K_m K_g}{R_a r} V_{aR} - \frac{J_{eq}}{r^2} \ddot{x} - H_{WR} \quad (4.21)$$

For the left wheel

The same way for calculation dynamic model for the left wheel to get

$$M_W \ddot{x} = \frac{-\eta_g \eta_m K_m K_g^2 K_c}{R_a r^2} \dot{x} + \frac{\eta_g \eta_m K_m K_g}{R_a r} V_{aL} - \frac{J_{eq}}{r^2} \ddot{x} - H_{WL} \quad (4.22)$$

Adding (4.21) and (4.22) together yields

$$2 \left(M_W + \frac{J_{eq}}{r^2} \right) \ddot{x} = \frac{-2\eta_g \eta_m K_m K_g^2 K_c}{R_a r^2} \dot{x} + \frac{\eta_g \eta_m K_m K_g}{R_a r} (V_{aL} + V_{aR}) - (H_{WL} + H_{WR}) \quad (4.23)$$

4.3.2 Dynamic Model for the Chassis

The robot's chassis can be modeled as an inverted pendulum, Figure 4.5 shows the free body diagram of the chassis and the pendulum.

θ_p is angle of the pendulum or pitch angle(rad)

δ is yaw angle (rad)

M_p is mass of the pendulum (kg)

L is distance between the center of the wheel and the robot's center of gravity (m)

D is lateral distance between the contact patches of the wheels (m)

We simplified the diagram with the sum of force for the pendulum Figure 4.6 and by using Newton's law of motion, summing the forces in the free body diagram of the pendulum in the horizontal direction to get

$$\begin{aligned}M_p \ddot{x} &= \sum F_{xP} \\ M_p \ddot{x} &= (H_{WL} + H_{WR}) - M_p L \ddot{\theta}_p \cos \theta_p + M_p L \dot{\theta}_p^2 \sin \theta_p\end{aligned}$$

$$M_P \ddot{y} = (V_{WL} + V_{WR}) - M_P g \quad (4.25)$$

Summing the forces perpendicular to the pendulum, we get

$$M_P \cos \theta_P \ddot{x} = \sum F_{xP}$$

$$M_P \cos \theta_P \ddot{x} = (H_{WL} + H_{WR}) \cos \theta_P + (V_{WL} + V_{WR}) \sin \theta_P - M_P g \sin \theta_P - M_P L \ddot{\theta}_P \quad (4.26)$$

Summing the moments around the centroid of the pendulum, we have

$$\begin{aligned} J_\alpha &= \sum M_O \\ J_P \ddot{\theta}_P &= -(H_{WL} + H_{WR}) L \cos \theta_P - (V_{WL} + V_{WR}) L \sin \theta_P - (C_{WL} + C_{WR}) \end{aligned} \quad (4.27)$$

where J_P is moment of inertia of the pendulum with respect to z axis.

Summing the moments for rotating the pendulum, we obtain

$$J_{P\delta} \ddot{\delta} = (H_{WL} - H_{WR}) \frac{D}{2} \quad (4.28)$$

where $J_{P\delta}$ is moment of inertia of the pendulum with respect to y axis.

Subtracting the reaction forces of the left wheel and the right wheel, we get

$$H_{WL} - H_{WR} = H_{TL} - H_{TR} \quad (4.29)$$

Subtracting the friction forces of the left wheel and the right wheel, we get

$$H_{TL} - H_{TR} = \frac{C_{WL} - C_{WR}}{R} \quad (4.30)$$

Rearranging (4.28), (4.29) and (4.30), we get

$$J_{P\delta} \ddot{\delta} = \left(\frac{C_{WL}}{R} - \frac{C_{WR}}{R} \right) \frac{D}{2} \quad (4.31)$$

Substitute (4.12) into (4.31) yields

$$J_{P\delta} \ddot{\delta} = \frac{\eta_g \eta_m K_m K_g D}{2 R_a r^2} (V_{aL} - V_{aR}) \quad (4.32)$$

Summing the torque applied on the pendulum from the two motors as defined in equation (4.12) and after a linear transformation

$$C_{WL} + C_{WR} = \frac{\eta_g \eta_m K_m K_g}{R_a} (V_{aL} + V_{aR}) - \frac{2 \eta_g \eta_m K_m K_g^2 K_c}{R_a r} \dot{x} \quad (4.33)$$

Substitute (4.33) into (4.27) and rearrange the equation yield

$$-(H_{WL} + H_{WR})L \cos \theta_P - (V_{WL} + V_{WR})L \sin \theta_P = J_P \ddot{\theta}_P + \frac{\eta_g \eta_m K_m K_g}{R_a} (V_{aL} + V_{aR}) - \frac{2\eta_g \eta_m K_m K_g^2 K_c}{R_a r} \dot{x} \quad (4.34)$$

Multiply equation (4.26) by $-L$ to get

$$[-(H_{WL} + H_{WR})L \cos \theta_P - (V_{WL} + V_{WR})L \sin \theta_P] + M_P g L \sin \theta_P + M_P L^2 \ddot{\theta}_P = -M_P L \cos \theta_P \ddot{x} \quad (4.35)$$

Substituting (4.34) into (4.35), we get

$$J_P \ddot{\theta}_P + \frac{\eta_g \eta_m K_m K_g}{R_a} (V_{aL} + V_{aR}) - \frac{2\eta_g \eta_m K_m K_g^2 K_c}{R_a r} \dot{x} + M_P g L \sin \theta_P + M_P L^2 \ddot{\theta}_P = -M_P L \cos \theta_P \ddot{x} \quad (4.36)$$

Eliminate $(H_{WR} + H_{WL})$ from the motor dynamics and substitute (4.24) into (4.23) to get,

$$2 \left(M_W + \frac{J_{eq}}{r^2} \right) \ddot{x} = \frac{-2\eta_g \eta_m K_m K_g^2 K_c \dot{x}}{R_a r^2} + \frac{\eta_g \eta_m K_m K_g (V_{aL} + V_{aR})}{R_a r} - M_P \ddot{x} - M_P L \ddot{\theta}_P \cos \theta_P + M_P L \dot{\theta}_P^2 \sin \theta_P \quad (4.37)$$

Rearranging (4.36) and (4.37) gives the nonlinear equations of motion of the system for balancing the pendulum

$$\ddot{\theta}_P = \frac{-M_P L \cos \theta_P \ddot{x}}{J_P + M_P L^2} + \frac{2\eta_g \eta_m K_m K_g^2 K_c \dot{x}}{R_a r (J_P + M_P L^2)} - \frac{M_P g L \sin \theta_P}{J_P + M_P L^2} - \frac{\eta_g \eta_m K_m K_g (V_{aL} + V_{aR})}{R_a (J_P + M_P L^2)} \quad (4.38)$$

$$\ddot{x} = \frac{-2\eta_g \eta_m K_m K_g^2 K_c \dot{x}}{R_a r^2 \left(2M_W + \frac{2J_{eq}}{r^2} + M_P \right)} + \frac{\eta_g \eta_m K_m K_g (V_{aL} + V_{aR})}{R_a r \left(2M_W + \frac{2J_{eq}}{r^2} + M_P \right)} - \frac{M_P L \ddot{\theta}_P \cos \theta_P}{2M_W + \frac{2J_{eq}}{r^2} + M_P} + \frac{M_P L \dot{\theta}_P^2 \sin \theta_P}{2M_W + \frac{2J_{eq}}{r^2} + M_P} \quad (4.39)$$

and the equation for the rotation for the MIP

$$\ddot{\delta} = \frac{\eta_g \eta_m K_m K_g D}{2J_{P\delta} R_a r^2} (V_{aL} - V_{aR}) \quad (4.40)$$

In the model above, it is assumed that the wheels of the vehicle always stay in contact with the ground and that there is no slip at the wheels.

4.4 Linearization

The above two equations can be linearized by assuming $\theta_P = \pi + \phi_P$, where ϕ_P represents a small angle from the vertical upward direction. This simplification is used so that a linear model can be obtained and linear state space controllers could be implemented. Therefore,

$$\cos \theta_P = -1, \quad \sin \theta_P = -\phi_P, \quad \text{and} \quad \left(\frac{d\theta_P}{dt} \right)^2 \approx 0$$

The linearized equation of motion is,

$$\ddot{\phi}_P = \frac{M_P L \ddot{x}}{J_P + M_P L^2} + \frac{2\eta_g \eta_m K_m K_g^2 K_c \dot{x}}{R_a r (J_P + M_P L^2)} + \frac{M_P g L \phi_P}{J_P + M_P L^2} - \frac{\eta_g \eta_m K_m K_g (V_{aL} + V_{aR})}{R_a (J_P + M_P L^2)} \quad (4.41)$$

$$\ddot{x} = \frac{-2\eta_g \eta_m K_m K_g^2 K_c \dot{x}}{R_a r^2 \left(2M_W + \frac{2J_{ca}}{r^2} + M_P \right)} + \frac{\eta_g \eta_m K_m K_g (V_{aL} + V_{aR})}{R_a r \left(2M_W + \frac{2J_{ca}}{r^2} + M_P \right)} + \frac{M_P L \ddot{\phi}_P}{2M_W + \frac{2J_{ca}}{r^2} + M_P} \quad (4.42)$$

In order to get the state-space representation of the system, equations (4.41) and (4.42) are rearranged

$$\ddot{\phi}_P = \frac{2\eta_g \eta_m K_m K_g^2 K_c (r\beta - M_P L) \dot{x}}{R_a r^2 \alpha} + \frac{\eta_g \eta_m K_m K_g (M_P L - r\beta) (V_{aL} + V_{aR})}{R_a r \alpha} + \frac{M_P g L \beta \phi_P}{\alpha} \quad (4.43)$$

$$\ddot{x} = \frac{2\eta_g \eta_m K_m K_g^2 K_c (M_P L r - J_P - M_P L^2) \dot{x}}{R_a r^2 \alpha} + \frac{(M_P L)^2 g \phi_P}{\alpha} + \frac{\eta_g \eta_m K_m K_g (-M_P L r + J_P + M_P L^2) (V_{aL} + V_{aR})}{R_a r \alpha} \quad (4.44)$$

where $\beta = 2M_W + \frac{2J_{ca}}{r^2} + M_P$, and $\alpha = J_P \beta + 2M_P L^2 \left(M_W + \frac{J_{ca}}{r^2} \right)$

The state-space equation for the system is obtained

$$\begin{pmatrix} \dot{x} \\ \ddot{x} \\ \dot{\phi}_P \\ \ddot{\phi}_P \\ \dot{\delta} \\ \ddot{\delta} \end{pmatrix} = \begin{pmatrix} 0 & 1 & 0 & 0 & 0 & 0 \\ 0 & \frac{2\eta_g \eta_m K_m K_g^2 K_c (M_P L r - J_P - M_P L^2)}{R_a r^2 \alpha} & \frac{(M_P L)^2 g}{\alpha} & 0 & 0 & 0 \\ 0 & 0 & 0 & 1 & 0 & 0 \\ 0 & \frac{2\eta_g \eta_m K_m K_g^2 K_c (r\beta - M_P L)}{R_a r^2 \alpha} & \frac{M_P g L \beta}{\alpha} & 0 & 0 & 0 \\ 0 & 0 & 0 & 0 & 0 & 1 \\ 0 & 0 & 0 & 0 & 0 & 0 \end{pmatrix} \begin{pmatrix} x \\ \dot{x} \\ \phi_P \\ \dot{\phi}_P \\ \delta \\ \dot{\delta} \end{pmatrix} + \begin{pmatrix} 0 & 0 \\ \frac{\eta_g \eta_m K_m K_g (-M_P L r + J_P + M_P L^2)}{R_a r \alpha} & \frac{\eta_g \eta_m K_m K_g (-M_P L r + J_P + M_P L^2)}{R_a r \alpha} \\ 0 & 0 \\ \frac{\eta_g \eta_m K_m K_g (M_P L - r\beta)}{R_a r \alpha} & \frac{\eta_g \eta_m K_m K_g (M_P L - r\beta)}{R_a r \alpha} \\ 0 & 0 \\ \frac{\eta_g \eta_m K_m K_g D}{2J_{P\delta} R_a r^2} & \frac{-\eta_g \eta_m K_m K_g D}{2J_{P\delta} R_a r^2} \end{pmatrix} \begin{pmatrix} V_{aL} \\ V_{aR} \end{pmatrix} \quad (4.45)$$

Cornering forces is also considered negligible.

Variables of the MIP are as in Table 4.1-4.3.

Table 4.1: Pendulum's variables.

Symbols	Values	Units
g : Gravity constant	9.81	m/s ²
r : Radius of the wheels	0.093	m
M_W : Mass of the wheels	1.282	kg
M_P : Mass of the pendulum	9.6	kg
J_W : Wheel moment of inertia	0.0111	kg-m ²
J_P : Pendulum moment of inertia respect to X axis	0.36	kg-m ²
$J_{P\delta}$: Pendulum moment of inertia respect to Z axis	0.563	kg-m ²
L : Length of center of the pendulum to cg	0.152	m
D : Lateral distance between the contact patches of the wheels	0.35	m

Table 4.2: Motor's variables.

Symbols	Values	Units
K_m : Motor-torque constant	0.0333	N-m/A
K_e : Back-emf constant	0.0333	V-s/rad
R_a : Motor armature resistance	0.62	Ω
η_m : Motor efficiency	85	%
J_m : Motor moment of inertia	0.000635	kg-m ²

Table 4.3: Gear's variables.

Symbols	Values	Units
η_g : Gearbox efficiency	80	%
K_g : Gear ratio	23	

Thus, the state-space equation becomes

$$\begin{pmatrix} \dot{x} \\ \ddot{x} \\ \dot{\phi}_P \\ \ddot{\phi}_P \\ \dot{\delta} \\ \ddot{\delta} \end{pmatrix} = \begin{pmatrix} 0 & 1 & 0 & 0 & 0 & 0 \\ 0 & -9.67 & 1.95 & 0 & 0 & 0 \\ 0 & 0 & 0 & 1 & 0 & 0 \\ 0 & -0.33 & 20.63 & 0 & 0 & 0 \\ 0 & 0 & 0 & 0 & 0 & 1 \\ 0 & 0 & 0 & 0 & 0 & 0 \end{pmatrix} \begin{pmatrix} x \\ \dot{x} \\ \phi_P \\ \dot{\phi}_P \\ \delta \\ \dot{\delta} \end{pmatrix} + \begin{pmatrix} 0 & 0 \\ 0.59 & 0.59 \\ 0 & 0 \\ 0.02 & 0.02 \\ 0 & 0 \\ 30.19 & -30.19 \end{pmatrix} \begin{pmatrix} V_{aL} \\ V_{aR} \end{pmatrix} \quad (4.46)$$

The eigenvalues of the balancing model are 0, -9.6769 , 4.5371 and -4.5284 . This means that the dynamic of this system near the point $\theta = 180^\circ$ is unstable.

Next we will find the linearized model using the operation point $\theta = 0^\circ$ to compare the dynamic with the nonlinear model. Similarly,

$$\cos \theta_P = 1, \quad \sin \theta_P = \phi_P, \quad \text{and} \quad \left(\frac{d\theta_P}{dt} \right)^2 \approx 0$$

The linearized equation of motion is

$$\ddot{\phi}_P = \frac{-M_P L \ddot{x}}{J_P + M_P L^2} + \frac{2\eta_g \eta_m K_m K_g^2 K_c \dot{x}}{R_a r (J_P + M_P L^2)} - \frac{M_P g L \phi_P}{J_P + M_P L^2} - \frac{\eta_g \eta_m K_m K_g (V_{aL} + V_{aR})}{R_a (J_P + M_P L^2)} \quad (4.47)$$

$$\ddot{x} = \frac{-2\eta_g \eta_m K_m K_g^2 K_c \dot{x}}{R_a r^2 \left(2M_W + \frac{2J_{eq}}{r^2} + M_P \right)} + \frac{\eta_g \eta_m K_m K_g (V_{aL} + V_{aR})}{R_a r \left(2M_W + \frac{2J_{eq}}{r^2} + M_P \right)} - \frac{M_P L \ddot{\phi}_P}{2M_W + \frac{2J_{eq}}{r^2} + M_P} \quad (4.48)$$

In order to get the state-space representation of the system, equations (4.47) and (4.48) are rearranging as

$$\ddot{\phi}_P = \frac{2\eta_g \eta_m K_m K_g^2 K_c (r\beta + M_P L) \dot{x}}{R_a r^2 \alpha} - \frac{\eta_g \eta_m K_m K_g (M_P L + r\beta) (V_{aL} + V_{aR})}{R_a r \alpha} - \frac{M_P g L \beta \phi_P}{\alpha} \quad (4.49)$$

$$\ddot{x} = \frac{-2\eta_g \eta_m K_m K_g^2 K_c (M_P L r + J_P + M_P L^2) \dot{x}}{R_a r^2 \alpha} + \frac{(M_P L)^2 g \phi_P}{\alpha} + \frac{\eta_g \eta_m K_m K_g (M_P L r + J_P + M_P L^2) (V_{aL} + V_{aR})}{R_a r \alpha} \quad (4.50)$$

where $\beta = 2M_W + \frac{2J_{eq}}{r^2} + M_P$, and $\alpha = J_P \beta + 2M_P L^2 \left(M_W + \frac{J_{eq}}{r^2} \right)$

The state-space equation for the system is obtained

$$\begin{pmatrix} \dot{x} \\ \ddot{x} \\ \dot{\phi}_P \\ \ddot{\phi}_P \\ \dot{\delta} \\ \ddot{\delta} \end{pmatrix} = \begin{pmatrix} 0 & 1 & 0 & 0 & 0 & 0 \\ 0 & \frac{-2\eta_g \eta_m K_m K_g^2 K_c (M_P L r + J_P + M_P L^2)}{R_a r^2 \alpha} & \frac{(M_P L)^2 g}{\alpha} & 0 & 0 & 0 \\ 0 & 0 & 0 & 1 & 0 & 0 \\ 0 & \frac{2\eta_g \eta_m K_m K_g^2 K_c (r\beta + M_P L)}{R_a r^2 \alpha} & \frac{-M_P g L \beta}{\alpha} & 0 & 0 & 0 \\ 0 & 0 & 0 & 0 & 0 & 1 \\ 0 & 0 & 0 & 0 & 0 & 0 \end{pmatrix} \begin{pmatrix} x \\ \dot{x} \\ \phi_P \\ \dot{\phi}_P \\ \delta \\ \dot{\delta} \end{pmatrix} + \begin{pmatrix} 0 & 0 \\ \frac{\eta_g \eta_m K_m K_g (M_P L r + J_P + M_P L^2)}{R_a r \alpha} & \frac{\eta_g \eta_m K_m K_g (M_P L r + J_P + M_P L^2)}{R_a r \alpha} \\ 0 & 0 \\ \frac{-\eta_g \eta_m K_m K_g (M_P L + r\beta)}{R_a r \alpha} & \frac{-\eta_g \eta_m K_m K_g (M_P L + r\beta)}{R_a r \alpha} \\ 0 & 0 \\ \frac{\eta_g \eta_m K_m K_g D}{2J_{P\delta} R_a r^2} & \frac{-\eta_g \eta_m K_m K_g D}{2J_{P\delta} R_a r^2} \end{pmatrix} \begin{pmatrix} V_{aL} \\ V_{aR} \end{pmatrix} \quad (4.51)$$

Thus, the state-space equation becomes

$$\begin{pmatrix} \dot{x} \\ \ddot{x} \\ \dot{\phi}_P \\ \ddot{\phi}_P \\ \dot{\delta} \\ \ddot{\delta} \end{pmatrix} = \begin{pmatrix} 0 & 1 & 0 & 0 & 0 & 0 \\ 0 & -13.44 & 1.95 & 0 & 0 & 0 \\ 0 & 0 & 0 & 1 & 0 & 0 \\ 0 & 40.21 & -20.63 & 0 & 0 & 0 \\ 0 & 0 & 0 & 0 & 0 & 1 \\ 0 & 0 & 0 & 0 & 0 & 0 \end{pmatrix} \begin{pmatrix} x \\ \dot{x} \\ \phi_P \\ \dot{\phi}_P \\ \delta \\ \dot{\delta} \end{pmatrix} + \begin{pmatrix} 0 & 0 \\ 0.82 & 0.82 \\ 0 & 0 \\ -2.44 & -2.44 \\ 0 & 0 \\ 30.19 & -30.19 \end{pmatrix} \begin{pmatrix} V_{aL} \\ V_{aR} \end{pmatrix} \quad (4.52)$$

The eigenvalues of the balancing model are 0, -13.0259 , $-0.2060 + 3.9014i$ and $-0.2060 - 3.9014i$.

4.5 Model Validation Using Zero Input-Responses

The zero-input responses of the pendulum angle near the operating points $\phi_P(0) = 0.5$ rad in Figure 4.7 are examined. The responses of nonlinear model and linear model are exactly the same and similar to experimental data by considering magnitude and oscillation period of the response. However, the experimental responses converge more rapidly than those of the simulations due to the friction effect and nonlinearities such as deadzone at low velocities. The zero-input responses with initial condition $\phi_P(0) = 0.95$ rad are shown in Figure 4.8. In this case, The simulation of nonlinear model and linear model has some time delay and has a little amplitude difference but those responses are still similar to the response of experimental data.

4.6 Conclusions

This chapter shows how to find an accurate mathematical model of an MIP by using a Newtonian approach. Thereafter, linear model one is obtained by the linearization around specified operating points. The simulation results show that the derived model gives similar responses to those of the experimental data.

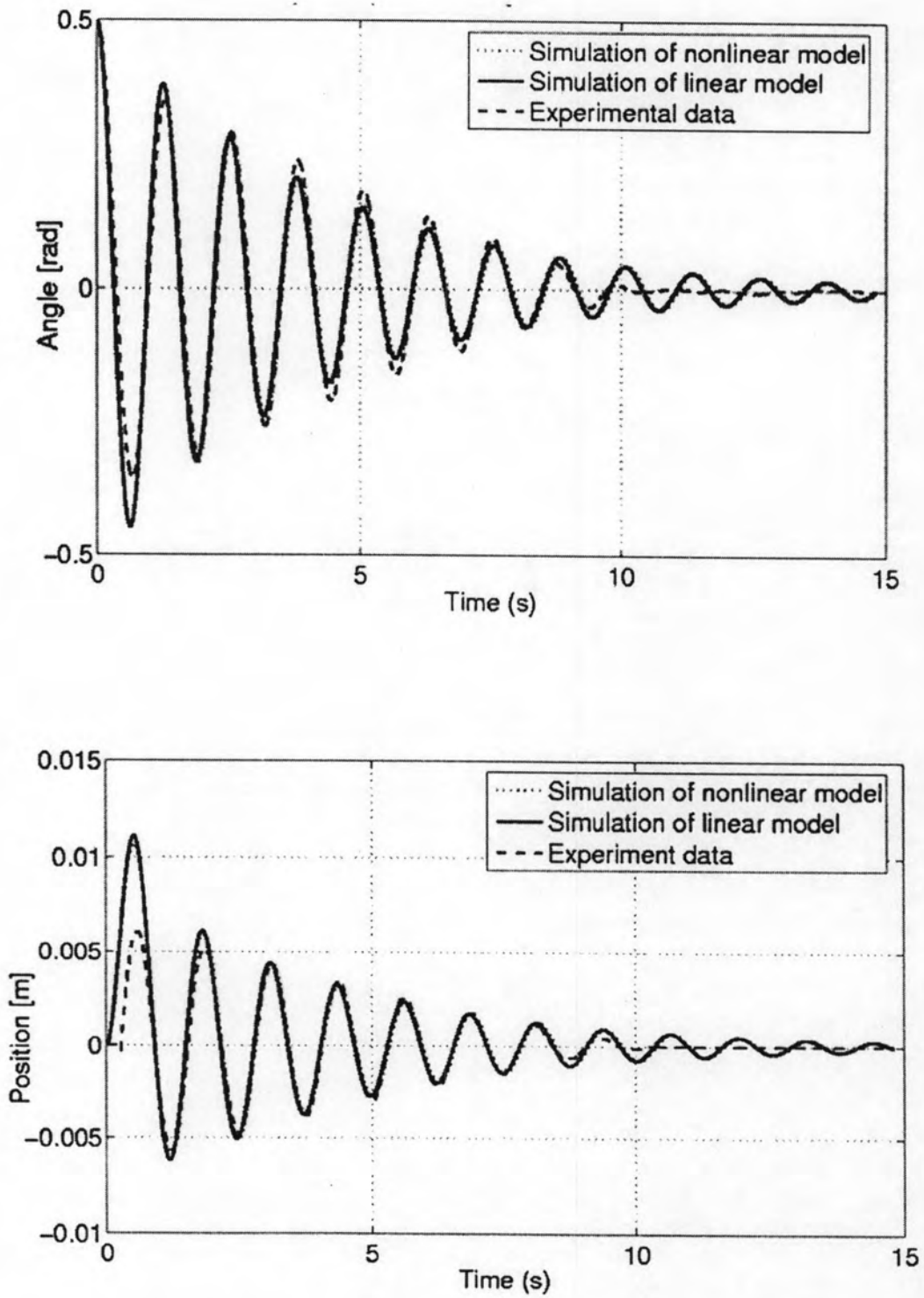


Figure 4.7: The zero-input response of angle and position when $\phi(0) = 0.5$ rad.

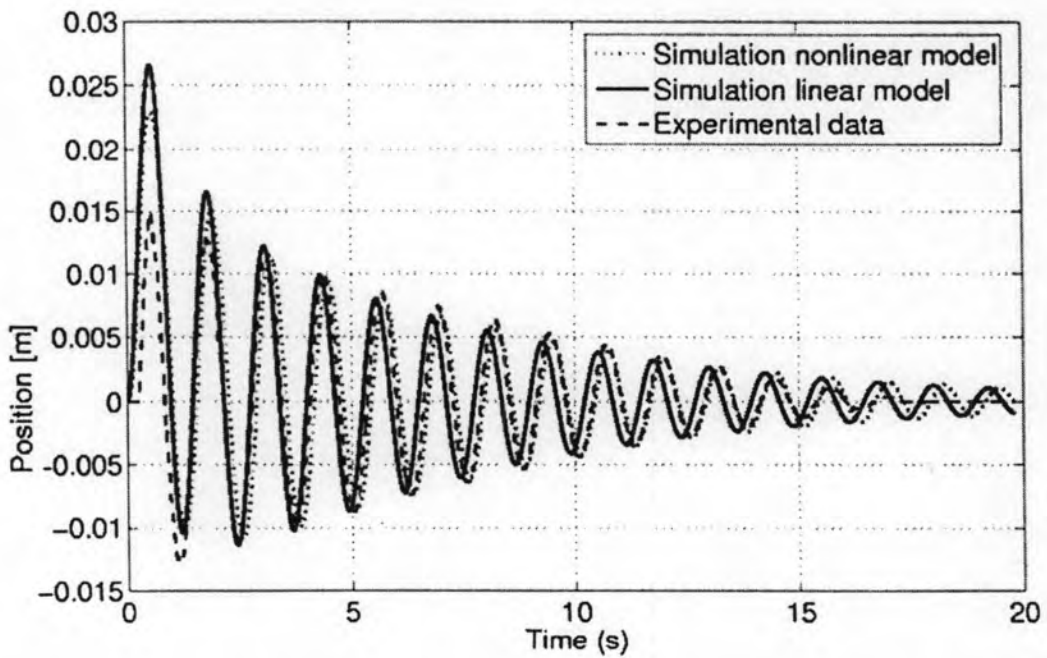
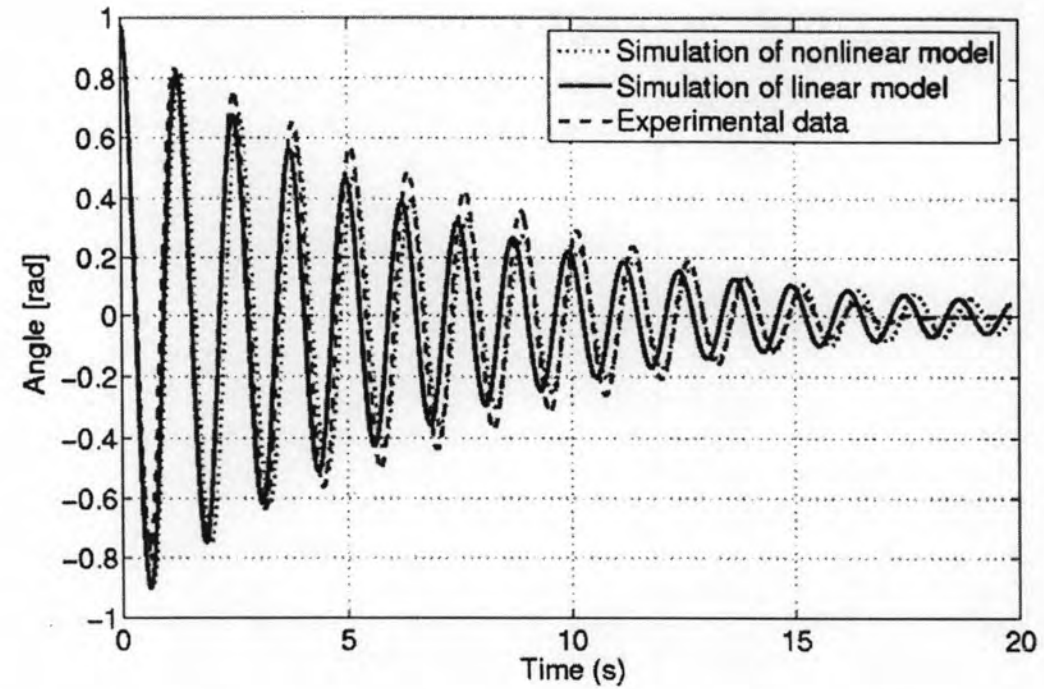


Figure 4.8: The zero-input response of angle and position when $\phi(0) = 0.95$ rad.